

Aerodynamic Parameter Estimation from Flight Data Applying Extended and Unscented Kalman Filter

Girish Chowdhary^{*} and Ravindra Jategaonkar[†]

DLR Institute for Flight Systems, Department of Systems Automation, Braunschweig, Germany.

Aerodynamic parameter estimation is an integral part of aerospace system design and life cycle process. Furthermore, recent advances in computational power have allowed the use of online parameter identification techniques in varied applications such as reconfigurable or adaptive control, system health monitoring, and fault tolerant control. The combined problem of state and parameter identification leads to a nonlinear filtering problem; furthermore, many aerospace systems are characterized by nonlinear identification models as well as noisy and biased sensor measurements. Extended Kalman Filter (EKF) is a commonly used algorithm for recursive parameter identification in the aerospace industry due to its excellent filtering properties and is based on a first order approximation of the system dynamics. Recently, the Unscented Kalman Filter (UKF) has been proposed as a theoretically better alternative to the EKF in the field of nonlinear filtering and has received great attention in navigation, parameter estimation, and dual estimation problems. The use of UKF as a recursive parameter estimation tool for aerodynamic modeling is relatively unexplored. In this paper we compare the performance of three recursive parameter estimation algorithms for aerodynamic parameter estimation of two aircraft from real flight data. We consider the EKF, the simplified version of the UKF and the augmented version of the UKF. The aircraft under consideration are a fixed wing aircraft (HFB-320) and a rotary wing UAV (ARTIS). The results indicate that although the UKF shows a slight improvement in some cases, the performance of the three algorithms remains comparable.

I. Introduction

PARAMETER estimation and System Identification techniques allow the engineer to form a mathematical model of a system using measured data. The Aerospace industry has placed great emphasis on system identification of various flight platforms since the resulting mathematical models are useful in the system design and management process, especially for the purpose of developing elaborate simulation environments and control systems design. System identification techniques can roughly be classified in two groups: offline techniques and online techniques. Offline system identification techniques tend to depend on iterative methods that exploit the advantage of having a complete set of data available for processing, whereas online or recursive system identification techniques must use the data as it becomes available. Recursive system identification is a valuable tool in the design of adaptive control laws^{e.g.1, 2}, health monitoring algorithms¹, and the design of fault tolerant systems⁶. Increasing availability of onboard computational power indicates further emergence of applications employing recursive parameter identification algorithms.

Recursive system identification techniques rely mainly on recursive parameter estimation, which handle flight data as it is measured through onboard sensors and estimate the required aerodynamic derivatives in real-time. Measured flight data can contain considerable amount of noise, furthermore there might be biases and unobserved states in the system model which must be estimated; hence filtering techniques are generally employed. Fundamental to all stochastic filtering methods is a two step Bayesian procedure¹⁹ consisting of prediction, or time update; and correction, or measurement update. The procedure developed by Kalman provides an optimal sequential linear state estimator which ideally suited for recursive implementations. The Kalman filter (Kalman 1960), which assumes Gaussian distribution for the uncertainties in system dynamics and utilizes the first two moments of the

^{*} Research Engineer, Lillienthalplatz 7, Braunschweig 38100 Germany, Member AIAA.

[†] Senior Scientist, Lillienthalplatz 7, Braunschweig 38100 Germany, Associate Fellow AIAA.

state vector (mean and covariance) in its update rule is an optimal sequential linear estimator ideally suited for recursive implementations. However, most aerospace systems involve a nonlinearity of some form, furthermore the state augmenting method of parameter estimation renders the filtering problem nonlinear, hence nonlinear filtering techniques must be employed.

The most popular nonlinear filtering technique in the aerospace industry is the Extended Kalman Filter (EKF), which employs instantaneous linearization at each time step to approximate the nonlinearities. The EKF can be hard to tune and implement when dealing with significant nonlinearities and exhibits divergence in extreme cases. Despite its theoretical shortcomings, however, the EKF has been employed successfully in various aircraft aerodynamic parameter estimation problems⁸⁻¹².

The problems associated with the EKF have been greatly attributed to the approximation introduced by the linearization⁷. The EKF approximates the mean and covariance using a first order approximation of the system dynamics. The Unscented Kalman Filter (UKF) overcomes these theoretical deficiencies by using a set of carefully selected sample points (also known as Sigma Points) to approximate the probability distribution of the random variable. The parameterized sets of sigma points are propagated through the nonlinear transformation and the mean and covariance of the transformed variables is used to approximate the mean and covariance of the sample space. Proper implementations of the UKF are accurate at least to the second order and do not require the computation of Jacobian or Hessian matrices. It is claimed that the computational complexity of the UKF is comparable to the EKF^{13,17}.

The UKF is based on the concept of Unscented Transforms (UT) introduced by Julier and Uhlmann¹³. In 14 Julier and Uhlmann demonstrate the feasibility and advantages of employing the UT in recursive filtering through the UKF for higher order nonlinear filtering problems such as reentry vehicle tracking. Their results indicate that UKF produces consistent estimates in situations where the EKF tends to produce inconsistent estimates. Wendel et al¹⁸ compare the performance of Sigma Point Kalman Filter (SPKF) with EKF for the nonlinear problem of tightly coupled GPS/INS integration. They report that owing to the moderate nonlinearities in their implementation of GPS-INS navigation equations both the EKF and the SPKF perform closely for all practical applications and recommend that modification of existing EKF based navigation systems may not result in significant performance improvement. Crassidis and Markley¹⁹ consider the UKF for spacecraft attitude estimation problems and report that for realistic conditions their UKF implementation consistently outperforms the EKF especially when large initialization errors are present. Brunke and Campbell²⁰ derive the elegant and robust square root sigma point filter and note that the SPKF is more amenable to online implementation. Brunke has also used the SPKF for aerodynamic parameter estimation in presence of a 50% stabilator failure. Wan and Van der Merwe study its extension to the problem of parameter estimation for selecting the weights of Neural Networks^{15,16}, the authors maintain that UKF consistently outperforms the EKF with comparable level of complexity.

The nonlinear dynamics of aerospace platforms and the presence of considerable noise and biases in measurements demand that a nonlinear filtering algorithm be used. Traditionally the EKF has been used for recursive parameter estimation purposes. In this paper we compare three recursive nonlinear filtering algorithms for aerodynamic parameter estimation from real flight data. The algorithms considered are, the EKF, the simplified version of the UKF which assumes additive white noise, and the augmented version of the UKF, which caters to the general case of noise entering the system nonlinearly. We analyze the feasibility and possible advantages of using the UKF for aircraft system identification from real flight data by comparing the results of UKF parameter estimation runs with results of EKF recursive estimation runs and offline estimation runs for two different types of aircraft. The two types of aircraft considered are a fixed wing platform (HFB 320) with nonlinear aerodynamic model and a miniature autonomous rotorcraft (ARTIS^{3,4}) with linearized state model.

II. Recursive Parameter Estimation for Aircraft

Estimation of parameters through the filtering approach is an indirect procedure, consisting of transforming the parameter estimation problem into a state estimation problem. This is done by augmenting the system state vector by artificially defining the unknown parameters as additional state variables. It is important to note that such a formulation will render the problem effectively nonlinear regardless whether a linear estimation model is used or otherwise. This nonlinearity manifests itself from state products.

To be as close to reality as possible a continuous estimation model is used, while to facilitate real-time application the measurements are recorded at discrete time steps and a discrete implementation of filtering algorithm is used. Such an approach which employs a continuous estimation model for prediction and a discrete filtering algorithm is known as the continuous-discrete filtering problem. The system dynamics are represented in generic continuous state space form along with the discrete measurement equation in Eq.(1),

$$\begin{aligned}
\dot{x}(t) &= f[x(t), u(t), \beta] + Fw(t), & x(t_0) &= x_0 \\
y(t) &= g[x(t), u(t), \beta] \\
z(k) &= y(k) + Gv(k), & k &= 1, \dots, N
\end{aligned} \tag{1}$$

Where x is the state vector having initial value x_0 at time t_0 , u is the input vector, y is the observation vector, Θ is the vector of unknown system parameters, f and g are the general nonlinear real-valued functions, z is the measurement vector sampled at N discrete time steps having a fixed sampling time of Δt and k is the discrete time index. The measurement noise vector V is assumed to be sequence of independent zero mean white Gaussian noise. The matrices F and G represent the additive state and measurement noise matrices and are considered to be time invariant.

The unknown parameter vector Θ consists of system parameters β , the measurement biases Δz , and the trim estimates formulated as input biases Δu^\dagger and is represented in Eq. (2).

$$\Theta^T = \{\beta^T; \Delta z^T; \Delta u^T\} \tag{2}$$

We consider the constant system parameters Θ as output of an auxiliary dynamic system presented in Eq. (3),

$$\dot{\Theta} = 0 \tag{3}$$

The augmented state vector is then defined in Eq. (5) as:

$$x_a = \begin{bmatrix} x \\ \Theta \end{bmatrix} \tag{4}$$

The extended system is represented in Eq. (6) as:

$$\begin{aligned}
\dot{x}_a(t) &= f_a[x_a(t), u(t)] + F_a W_a(t) \\
&= \begin{bmatrix} f[x(t), u(t), \beta] \\ 0 \end{bmatrix} + \begin{bmatrix} F & 0 \\ 0 & 0 \end{bmatrix} \begin{bmatrix} w(t) \\ 0 \end{bmatrix} \\
y(t) &= g_a[x_a(t), u(t)] \\
z(k) &= y(k) + Gv(k)
\end{aligned} \tag{5}$$

Where, the augmented variables are denoted by subscript “a”. The three algorithms that we consider are explained in this section.

A. The Extended Kalman Filter

For the augmented system of Eq. (5) the EKF consisting of an extrapolation (prediction) and an update step is summarized below^{10,23}. In what follows we use the notation “tilde” (\sim) and “hat” ($\hat{\cdot}$) to denote the predicted and corrected variables respectively.

Extrapolation:

[†] It may not be possible to estimate all the components of Δz and Δu since they could be linearly dependent or highly correlated¹⁰.

$$\tilde{x}_a(k) = \hat{x}_a(k-1) + \int_{t(k-1)}^{t(k)} f_a[\hat{x}_a(t), \bar{u}(k)] dt \quad (6)$$

$$\tilde{y}(k) = g_a[\tilde{x}_a(k), u(k)]$$

$$\tilde{P}_a(k) \approx \Phi_a(k) \hat{P}_a(k-1) \Phi_a^T(k) + \Delta t F_a F_a^T \quad (7)$$

With the initial conditions

$$\hat{x}_a(1) = x_{a0} \quad \hat{P}_a(1) = P_{a0} \quad (8)$$

\bar{u} denotes average or interpolated values of the inputs between points k-1 and k, and $\Phi_a = e^{A_a \Delta t}$ denotes the discrete time state transition matrix from the augmented system with,

$$A_a(k) = \frac{\partial f_a}{\partial x_a} \Big|_{x_a = \hat{x}_a(k-1)} = \begin{bmatrix} \frac{\partial f}{\partial x} & \frac{\partial f}{\partial \Theta} \\ 0 & 0 \end{bmatrix} \Big|_{x_a = \hat{x}_a(k-1)} \quad (9)$$

\bar{u} denotes average or interpolated values of the inputs between points k-1 and k. Eq. (9) denotes the linearization process for the state matrix. The linearization can be carried out using a numerical implementation of the central difference formula around the last best state estimate at each discrete time step^{10,23}.

Update:

$$\begin{aligned} K_a(k) &= \tilde{P}_a(k) C_a^T(k) [C_a(k) \tilde{P}_a(k) C_a^T(k) + G G^T]^{-1} \\ \hat{x}_a(k) &= \tilde{x}_a(k) + K_a(k) [z(k) - \tilde{y}(k)] \\ \hat{P}_a(k) &= [I - K_a(k) C_a(k)] \tilde{P}_a(k) \\ &= [I - K_a(k) C_a(k)] \tilde{P}_a(k) [I - K_a(k) C_a(k)]^T + K_a(k) G G^T K_a^T(k) \end{aligned} \quad (10)$$

Where $C_a(k)$ is the linearized measurement matrix as represented in Eq. (11), as before the linearization can be carried out using the central difference formula.

$$C_a(k) = \frac{\partial g_a}{\partial x_a} \Big|_{x_a = \tilde{x}_a(k)} = \begin{bmatrix} \frac{\partial g}{\partial x} & \frac{\partial g}{\partial \Theta} \end{bmatrix} \Big|_{x_a = \tilde{x}_a(k)} \quad (11)$$

The Runge-Kutta algorithm can be used for integration in Eq. (7), the state transition matrix Φ_a can be approximated using Padé approximation²³ or Taylor series expansion. $P_a(0)$ represents the confidence in the initial state estimates and must be specified a priori. In the absence of any a priori knowledge of the parameter values it is common to assume high values for the $P_a(0)$ matrix¹⁰. The value of FF^T and GG^T i.e. the process and measurement noise covariance matrices must also be specified a priori. The measurement noise covariance matrix GG^T can be calibrated using laboratory measurements of sensors to ensure good noise filtering. The process noise covariance matrix FF^T is however more difficult to determine and a trial and error method is employed if no other suitable method is found. We do not consider the problem of adaptive filtering in this paper, which attempts to adapt to the unknown noise characteristics²⁵.

The propagation of the covariance matrix P in Eq. (9) is a linear approximation for a small Δt . It ignores the higher order terms of the Taylor series expansion for propagating the covariance matrix. These ignored terms may contain higher order effects that affect the performance of the filter¹⁴. This makes the EKF a non-optimal

approximation of the KF based on a first order approximation of nonlinear dynamic system. The EKF exhibits better performance if the system under consideration is close to linear, whereas strong system nonlinearities and wrong values of noise statistics may result in biased estimates or in worst case lead to divergence²¹.

B. The Unscented Kalman Filter: augmented case

Various techniques have been proposed to address the inaccuracies arising from the fundamental first order approximation inherent to the EKF implementation. The continuous-discrete mixed approach which uses nonlinear model for propagation of the system states and a linearized model for propagation of the error covariance mitigates the problem somewhat, however the fundamental problem of not accounting for the nonlinear transformations that the random variable undergo remains, affecting the accuracy. Other techniques, such as the Iterated Kalman Filter, or second and higher order filters are possible and have shown good estimation error reduction in specific application areas; but these are found to be much more involved. Julier and Uhlmann^{13,14} introduced the concept of Unscented Transforms and extended it to the problem of recursive estimation. The resulting filter is known as the Unscented Kalman Filter (UKF).

The UKF is based on the idea that *it is easier to approximate a probability distribution than to approximate an arbitrary nonlinear transformation*¹⁴. The actual algorithm is based on propagating carefully selected finite set of points, called sigma points, through the system nonlinear dynamics, and then approximating the first two moments of the distribution (mean and covariance) through a suitable method; such as weighted sample mean and covariance calculations^{14,16}. The flaw in the EKF that results from propagating the mean and covariance through linear approximations of the nonlinear transformation is thus eliminated in the UKF, leading to theoretically better performance of the UKF. Furthermore, the UKF implementation does not need the calculation of any Jacobian or Hessian matrices, which not only results in considerable simplicity in implementation, but also makes the UKF suitable for real-time applications and applications involving non-differentiable functions. The accuracy of the UKF can be compared to that of the second order EKF, the computational order is comparable to the EKF^{14,16}.

The UKF algorithm requires the definition of $2n_a + 1$ sigma points, where n_a is the total number of states to be estimated, consisting of augmented system states with the unknown system parameters as well as the process and measurement noise disturbances. Each sigma point consists of a vector, one of the sigma vectors is the expected value of the augmented state vector and the remaining $2n_a$ points are obtained from the columns of the matrix square root $\pm(\gamma P)$ for $i=1,2,\dots,n_a$, where P is the covariance matrix of the augmented state vector x_a , and $\gamma = \alpha^2(n_a + \kappa) - n_a$ are scaling parameters. The constant α determines the spread of the sigma points around x_a and is usually set to small positive values less than one (typically in the range 0.001 to 1) whereas κ is the secondary scaling parameter usually set to zero or 3- n . When κ is set to zero, the sigma points and their weights are related to the dimension of the state vector directly (n), when κ is set to $\kappa=3-n$, the fourth order moment information is mostly captured in the true Gaussian case¹⁴. The weighted mean and covariance of the sigma points are captured in the following manner:

$$\begin{aligned} \sum_{i=1}^n w_i x_i &\approx \bar{x} \\ \sum_{i=1}^n w_i^m (x_i - \bar{x})(x_i - \bar{x})^T &\approx P_{xx} \end{aligned} \quad (12)$$

Where the weights W are calculated as:

$$\begin{aligned} W_0^m &= \lambda / (n_a + \lambda) \\ W_0^c &= \lambda / (n_a + \lambda) + (1 - \alpha^2 + \beta) \\ W_i^m &= W_i^c = 1 / \{2(n_a + \lambda)\}, \quad i = 1, 2, \dots, 2n_a \end{aligned} \quad (13)$$

where the subscript '0' corresponds to the estimated states and $i=1,2,\dots,2n_a$ the other sigma points; the superscripts 'm' and 'c' indicate weights for the computation of mean and covariance respectively. The constant β is used to incorporate prior knowledge of the distribution of x in the computation of weights for covariances W_0^c ; the

optimum value is $\beta=2$ for Gaussian distribution. The scale parameters may be tuned to match the specific problem; some guidelines to choose them are provided in 14.

To illustrate the UKF procedure, let us consider a discrete time representation widely used in the applications of the UKF. For the discrete time nonlinear state space model be given by:

$$x_{k+1} = f_d(x_k, \Theta_k, u_k, w_k) \quad (14)$$

$$y_k = g_d(x_k, \Theta_k, u_k, v_k) \quad (15)$$

where x_k is the $(n_x \times 1)$ state vector, Θ_k the $(n_q \times 1)$ vector of unknown parameters, u_k the $(n_u \times 1)$ vector of exogenous inputs, y_k the $(n_y \times 1)$ model output vector, f_d and g_d the corresponding state and output functions. In a general case, the process noise w_k and the measurement noise v_k are assumed to enter the model nonlinearly as implied by the Eqs.(14) and (15) and are $(n_w \times 1)$ and $(n_v \times 1)$ size vectors respectively. The measurement vector is denoted by z_k . The augmented state vector of the size $(n_a \times 1)$ is given by:

$$x_k^a = [x_k^T \quad \Theta_k^T \quad w_k^T \quad v_k^T]^T \quad (16)$$

where the superscript 'a' denotes the augmented state vector, $n_a = n_{xp} + n_w + n_v$ and $n_{xp} = n_x + n_q$. We consider cases where $n_w = n_{xp}$ and $n_v = n_y$. The noise processes w_k and v_k are assumed to be zero mean, and with covariance matrices Q and R respectively. The starting values of the augmented state vector and its covariance are given by:

$$\begin{aligned} \hat{x}_0^a &= E\{x_0^a\} = E\{[\hat{x}_0^T \quad \Theta_0^T \quad w_0^T \quad v_0^T]^T\} \\ &= [\hat{x}_0^T \quad \Theta_0^T \quad 0 \quad 0] \end{aligned} \quad (17)$$

$$P_0^a = E\{(x_0^a - \hat{x}_0^a)(x_0^a - \hat{x}_0^a)^T\} = \begin{bmatrix} P_{x0} & 0 & 0 & 0 \\ 0 & P_{\Theta 0} & 0 & 0 \\ 0 & 0 & Q & 0 \\ 0 & 0 & 0 & R \end{bmatrix}. \quad (18)$$

Following the guidelines already discussed, we choose the constants α , β , and the scaling parameters κ , γ and λ , and compute the set of weights W_i^m and W_i^c for $i=0,1,...,2n_a$. The UKF recursive estimation algorithm follows the standard Bayesian solution to continuous-discrete filtering problem consisting of a prediction and an update step²⁴. The prediction step predicts the probability density at time step t_k and the measurement step calculates the posterior probability density from the predicted probability density from the prediction step and the measurement y at time t_k .

The standard UKF algorithm can be summarized as follows¹⁷:

- 1) Set discrete time point $k=1$ and build up the augmented state vector \hat{x}_k^a and the corresponding covariance matrix \hat{P}_k^a for the initial values according to Eqs. (17) and (18) respectively.
- 2) Calculate the $(2n_a + 1)$ sigma points

$$\hat{\mathcal{X}}_k^a = \begin{bmatrix} \hat{x}_k^a & \hat{x}_k^a - \gamma \sqrt{\hat{P}_k^a} & \hat{x}_k^a + \gamma \sqrt{\hat{P}_k^a} \end{bmatrix} \quad (19)$$

- 3) Prediction (Time update):

$$\tilde{\chi}_{k+1}^a = f_d[\hat{\chi}_k^x, u_k, \hat{\chi}_k^w] \quad (20)$$

$$\tilde{x}_{k+1}^a = \sum_{i=0}^{2n_a} W_i^m \hat{\chi}_{i,k+1}^a \quad (21)$$

$$\tilde{P}_{k+1} = \sum_{i=0}^{2n_a} W_i^c [\tilde{\chi}_{i,k+1}^x - \tilde{x}_{k+1}] [\tilde{\chi}_{i,k+1}^x - \tilde{x}_{k+1}]^T \quad (22)$$

4) Measurement update:

$$\mathcal{Y}_{k+1} = g_d[\tilde{\chi}_{k+1}^x, u_{k+1}, \tilde{\chi}_{k+1}^v] \quad (23)$$

$$\tilde{y}_{k+1} = \sum_{i=0}^{2n_a} W_i^m \mathcal{Y}_{i,k+1} \quad (24)$$

$$P_{\tilde{y}\tilde{y}_{k+1}} = \sum_{i=0}^{2n_a} W_i^c [\mathcal{Y}_{i,k+1} - \tilde{y}_{k+1}] [\mathcal{Y}_{i,k+1} - \tilde{y}_{k+1}]^T \quad (25)$$

$$P_{\tilde{x}\tilde{y}_{k+1}} = \sum_{i=0}^{2n_a} W_i^c [\tilde{\chi}_{i,k+1}^x - \tilde{x}_{k+1}] [\mathcal{Y}_{i,k+1} - \tilde{y}_{k+1}]^T \quad (26)$$

$$K_{k+1} = P_{\tilde{x}\tilde{y}_{k+1}} P_{\tilde{y}\tilde{y}_{k+1}}^{-1} \quad (27)$$

$$\hat{x}_{k+1} = \tilde{x}_{k+1} + K_{k+1} (z_{k+1} - \tilde{y}_{k+1}) \quad (28)$$

$$\hat{P}_{k+1} = \tilde{P}_{k+1} - K_{k+1} P_{\tilde{y}\tilde{y}_{k+1}} K_{k+1}^T \quad (29)$$

5) Increment k and return to step 2 to continue to next time point.

In Eqs. (19) through (29), $\mathcal{X}^a = [(\mathcal{X}^x)^T (\mathcal{X}^w)^T (\mathcal{X}^v)^T]^T$ denotes the sigma points, \mathcal{X}^x corresponds to the system states and unknown parameters, ‘~’ (tilde) the predicted values, and ‘^’ (hat) the corrected values. The presented UKF algorithm is for the general discrete time case of noise entering nonlinearly into the system dynamics and is henceforth referred to as the augmented case²². A continuous estimation model is used as aircraft dynamics evolve naturally over time. Hence, similar to the presented EKF implementation, we use numerical integration methods to propagate the sigma points through the continuous nonlinear equations instead of eq. (20):

$$\tilde{x}_{k+1}^a = \hat{x}_k^a(k) + \int_{t_k}^{t_{k+1}} f[\chi^a(t), \bar{u}(k)] dt \quad (30)$$

Although the UKF bears some resemblance to particle filter algorithms, the main difference between UKF or SPKF algorithms and particle filter algorithms is that the sigma points are not drawn at random, but are carefully chosen to capture specific properties of the state variable distribution.

C. The Unscented Kalman Filter: Simplified case

For the continuous representation of nonlinear system dynamics with *additive* noise of eq (1) the UKF steps are very similar to those of Eqs. (19) to (29), but for the two modifications:

- 1) Propagation of sigma points through numerical integration, and
- 2) Simplification resulting from additive noise disturbances.

As in the case of EKF or the augmented UKF, we use numerical integration methods (Eq. 30) to propagate the sigma points through the continuous nonlinear equations instead of eq. (20). For additive zero-mean noise disturbances the augmentation of the state vector through noise vectors is not necessary. Hence the augmented state vector is given by $x_k^a = [x_k^T \quad \Theta_k^T]^T$, as in the case of EKF. Consequently, the initial covariance matrix P_0^a corresponds to that of the states and system parameters only, and the total number of states to be estimated is $n_a = n_{xp}$. The respective noise covariances Q and R are simply added to the right sides of Eqs. (22) and (25):

$$\tilde{P}_{k+1} = \sum_{i=0}^{2n_a} W_i^c [\tilde{\chi}_{i,k+1}^x - \tilde{x}_{k+1}] [\tilde{\chi}_{i,k+1}^x - \tilde{x}_{k+1}]^T + Q \quad (31)$$

$$P_{\tilde{y}\tilde{y}_{k+1}} = \sum_{i=0}^{2n_a} W_i^c [\mathcal{Y}_{i,k+1} - \tilde{y}_{k+1}] [\mathcal{Y}_{i,k+1} - \tilde{y}_{k+1}]^T + R \quad (32)$$

The reduced size of the augmented state vector and sigma points leads to a reduction in computational load. By comparing the UKF steps given above with those of the EKF in the previous section, it is seen that the major changes pertain to computing the mean and covariances of states and outputs; whereas the measurement update is basically similar. It is also apparent that the first or second-order approximations of the system dynamics are not required.

III. Application to flight vehicles: Fixed wing platform

Two different types of aircraft are considered. The first aircraft considered is a fixed wing research aircraft HFB-320.



Figure 1: The DLR HFB-320 research aircraft

We estimate the lift, drag, and pitching moment coefficients of the research aircraft HFB-320. Flight tests were carried out to excite the longitudinal motion through a multi-step elevator input resulting in short period motion and a pulse input leading to phugoid motion.²⁸ The following model is used to estimate the non-dimensional derivatives:

State equations:

$$\begin{aligned}\dot{V} &= -\frac{\bar{q}S}{m} C_D + g \sin(\alpha - \theta) + \frac{F_e}{m} \cos(\alpha + \sigma_T) \\ \dot{\alpha} &= -\frac{\bar{q}S}{mV} C_L + q + \frac{g}{V} \cos(\alpha - \theta) - \frac{F_e}{mV} \sin(\alpha + \sigma_T) \\ \dot{\theta} &= q \\ \dot{q} &= \frac{\bar{q}S\bar{c}}{I_y} C_m + \frac{F_e}{I_y} (\ell_{tx} \sin \sigma_T + \ell_{tz} \cos \sigma_T)\end{aligned}\tag{33}$$

where the lift, drag, and pitching moment coefficients are modeled as:

$$\begin{aligned}C_D &= C_{D0} + C_{DV} \frac{V}{V_0} + C_{D\alpha} \alpha \\ C_L &= C_{L0} + C_{LV} \frac{V}{V_0} + C_{L\alpha} \alpha \\ C_m &= C_{m0} + C_{mV} \frac{V}{V_0} + C_{m\alpha} \alpha + C_{mq} \frac{q\bar{c}}{2V_0} + C_{m\delta_e} \delta_e\end{aligned}\tag{34}$$

Observation equations:

$$\begin{aligned}V_m &= V \\ \alpha_m &= \alpha \\ \theta_m &= \theta \\ q_m &= q \\ \dot{q}_m &= \frac{\bar{q}S\bar{c}}{I_y} C_m + \frac{F_e}{I_y} (\ell_{tx} \sin \sigma_T + \ell_{tz} \cos \sigma_T) \\ a_{xm} &= \frac{\bar{q}S}{m} C_X + \frac{F_e}{m} \cos \sigma_T \\ a_{zm} &= \frac{\bar{q}S}{m} C_Z - \frac{F_e}{m} \sin \sigma_T\end{aligned}\tag{35}$$

where the longitudinal and vertical force coefficients C_X and C_Z are given by:

$$\begin{aligned}C_X &= C_L \sin \alpha - C_D \cos \alpha \\ C_Z &= -C_L \cos \alpha - C_D \sin \alpha\end{aligned}\tag{36}$$

where V is the true airspeed, α the angle of attack, θ the pitch attitude, q the pitch rate, δ_e the elevator deflection, F_e the thrust, σ_T the inclination angle of the engines, $\bar{q} (=1/2 \rho V^2)$ the dynamic pressure, m the mass, S the wing area, \bar{c} the wing chord, I_y the moment of inertia, and ρ the density of air. The subscript m on the right hand side of Eq. (35) denotes the measured quantities. These system equations in terms of variables in the stability axes (V , α) contain not only the common trigonometric and multiplicative nonlinearities, but in addition,

the variable dynamic pressure $\bar{q} (=1/2 \rho V^2)$, which multiplies all of the aerodynamic derivatives, introduces an additional nonlinearity. Furthermore, inversion of the state variable V leads to further nonlinearities in the state equation for α . Flight tests were carried out to excite the longitudinal motion through a multi-step elevator input resulting in short period motion and a pulse input leading to phugoid motion²⁸. The unknown parameter vector Θ consisting of the non-dimensional derivatives is given by:

$$\Theta = [C_{D0} \ C_{DV} \ C_{D\alpha} \ C_{L0} \ C_{LV} \ C_{L\alpha} \ C_{m0} \ C_{mV} \ C_{m\alpha} \ C_{mq} \ C_{m\delta_e}]^T \quad (37)$$

The filtering performance is seen in Figure 2. Figure 3 compares the performance of the three recursive parameter estimation methods for the purpose of aerodynamic parameter estimation. It is clearly seen that the parameter estimates of all these methods are in close vicinity of one another. Furthermore, excellent agreement is seen between the recursive parameter estimation method and the offline Filter Error Method (FEM) estimates of the parameters.

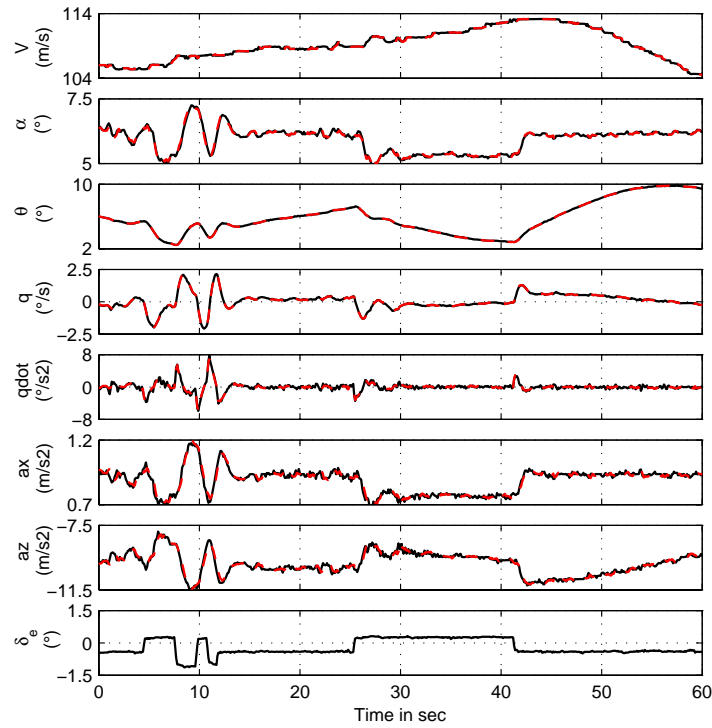


Figure 2 Time history for HBF 320

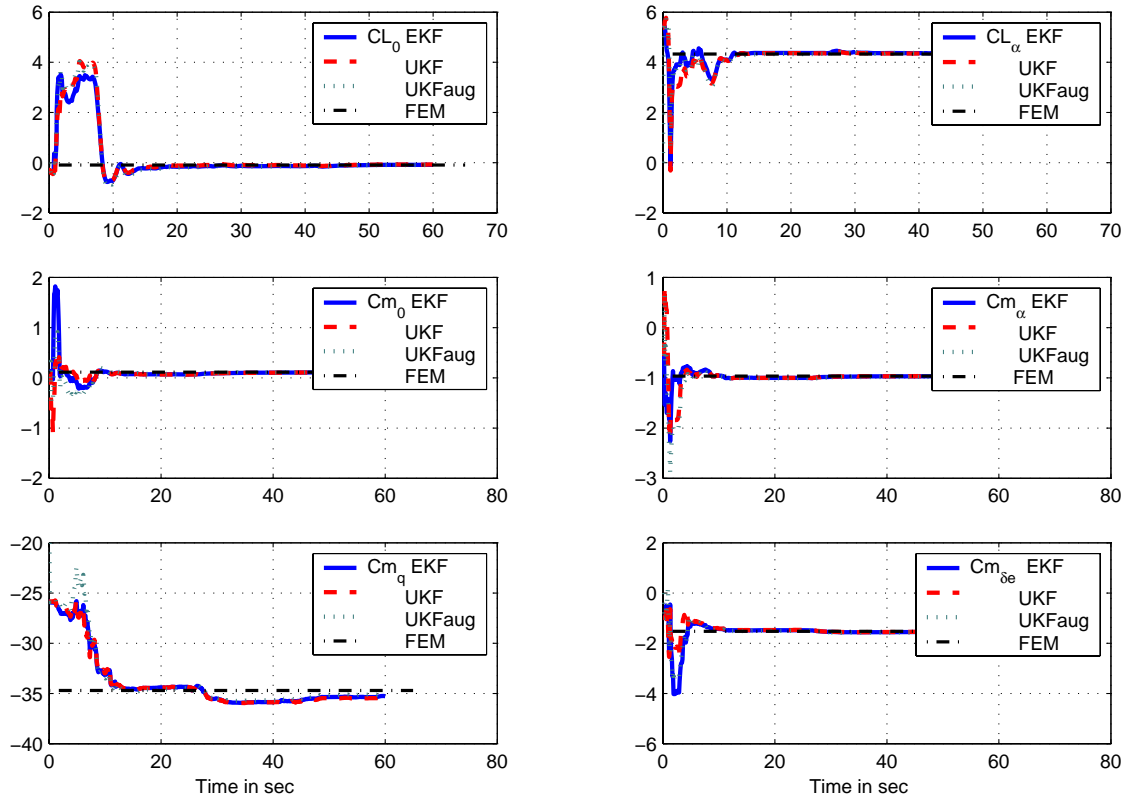


Figure 3: Performance of recursive parameter estimation methods for aerodynamic parameter identification of the research aircraft HFB-320

Table 1: Comparison of parameter estimates for the HFB-320

Parameter	Filter error method (FEM)	<i>RPE methods</i>		
		<i>EKF</i>	<i>UKF</i>	<i>UKFaug</i>
C_{D0}	0.123 (2.45)*	0.124 (2.49)	0.123 (2.58)	0.124 (2.50)
C_{DV}	-0.0645 (3.95)	-0.0657 (3.98)	-0.0648 (4.15)	-0.0659 (3.98)
$C_{D\alpha}$	0.320 (2.26)	0.319 (2.32)	0.320 (2.39)	0.316 (2.37)
C_{L0}	-0.0929 (21.1)	-0.0875 (23.1)	-0.760 (26.5)	-0.909 (22.1)
C_{LV}	0.149 (11.1)	0.147 (11.5)	0.137 (12.4)	0.150 (11.2)
$C_{L\alpha}$	4.328 (1.08)	4.292 (1.14)	4.287 (1.15)	4.294 (1.14)
C_{m0}	0.112 (3.27)	0.112 (4.25)	0.111 (4.27)	0.115 (3.40)
C_{mV}	0.0039 (82.1)	0.0041 (100)	0.0044 (93.6)	0.0022 (157)
$C_{m\alpha}$	-0.968 (1.12)	-0.969 (1.54)	-0.968 (1.54)	-0.982 (1.24)
C_{mq}	-34.710 (2.27)	-35.263 (2.82)	-35.380 (2.82)	-35.027 (2.27)
$C_{m\delta e}$	-1.529 (1.27)	-1.538 (1.64)	-1.536 (1.65)	-1.549 (1.31)

(*the values in parenthesis denote standard deviation values in percent.)

The excellent performance of all the methods and their close agreement can largely be attributed to an accurate mathematical model of the system under consideration. Table 1 compares the numerical values of the estimates of the parameters arrived at with the different methods. All numerical values are in excellent agreement.

IV. Application to flight vehicles: Rotary wing platform

The second aircraft considered in this paper is a rotary wing aircraft: ARTIS^{1,3,4} (Autonomous Rotorcraft Testbed for Intelligent Systems) which is an Unmanned Aerial Vehicle (UAV). The ARTIS is based on a commercially available miniature rotorcraft flight platform that is often used for acrobatic flight by miniature helicopter pilots. The baseline vehicle is a modified Benda Genesis 1800 helicopter. Due to the extreme maneuverability and a very high thrust-to-weight ratio of the flight platform, the instrumented UAV is able to fly even the most dynamic and aggressive maneuvers. A multi-sensor navigation system based on off the shelf sensors has been developed for ARTIS which provides optimized navigation solutions using sensor fusion techniques. The avionics suite is designed in a modular way, detailed information on the avionics suite can be found in reference 3 and 4.



Figure 4: The ARTIS VTOL UAV

A linear estimation model is used which is valid for the rotorcrafts hover domain. Sequences of frequency sweep inputs are used for the purpose of flight data collection as these provide a very rich set of estimation data for the inherently unstable UAV platform^{3,26}.

The system state and observation equations are modeled as:

$$\begin{aligned} \dot{x}(t) &= Ax(t) + B(u(t) + \Delta u_{trim}), & x(t_0) &= x_0 \\ y &= Cx(t) + \Delta z \end{aligned} \quad (38)$$

Where the system matrix A , the input matrix B and the measurement matrix C are functions of parameters to be identified β and $\beta = [\beta_A; \beta_B; \beta_C]$. Extended states Δu_{trim} and Δz represent the respective input and measurement biases to be identified. The state vector x consists of u , v and w which are the rotorcraft velocities in body x , y and z axes respectively, p , q and r which are the rotorcraft angular rates around the body x , y and z axes respectively. ϕ and θ which are the Euler angles as well as a and b which are respectively rotorcraft internal states for longitudinal and lateral rotor flapping angles. Sensor measurements are available for all the velocities, angular rates and Euler angles, however they may contain noise and sensor biases. The internal states a and b are not measured and must be estimated. It is important to note that the system model is time variant in the true sense and the parameters as well as the trim and output bias values are not constant, rather, are functions of time. However, for the purpose of this paper we will consider a time invariant model trimmed around the hover domain. For linear

representation of rotorcraft systems the measurement matrix C usually equates measurements directly to states, in this case the estimation problem is simplified as the number of parameters to be estimated is reduced.

The recorded pilot input for the identification maneuvers performed are shown in Figure 5, the maneuvers consist of variable frequency input sweeps on the lateral cyclic and the longitudinal cyclic inputs and are executed manually through a remote control by a trained pilot. The sensor measurements are corrupted by noise and vibrations of the rotorcraft frame, furthermore the measurements may contain a considerable amount of process noise which is accounted to windy conditions of the day of the flight test. Apart from these 6 parameters, 4 input trims (one on each input), and two biases (on phi and theta Euler angles) are also estimated. We pay special attention to the performance of the filter in estimating states, filtering noise, and estimating parameters in order to assess the feasibility of the filter to be used in recursive state and parameter estimation applications¹. The estimates acquired from recursive parameter methods are compared to offline estimation runs undertaken using the output error method for the same set of data.

The rotorcraft State and input matrices are given as:

$$\begin{bmatrix} \dot{u} \\ \dot{v} \\ \dot{p} \\ \dot{q} \\ \dot{a} \\ \dot{b} \\ \dot{w} \\ \dot{r} \\ \dot{\phi} \\ \dot{\theta} \end{bmatrix} = \begin{bmatrix} X_u & 0 & 0 & 0 & X_a & 0 & 0 & 0 & 0 & -g \\ 0 & Y_v & 0 & 0 & 0 & Y_b & 0 & 0 & g & 0 \\ L_u & L_v & 0 & 0 & 0 & L_b & L_w & 0 & 0 & 0 \\ M_u & M_v & 0 & 0 & M_a & 0 & M_w & 0 & 0 & 0 \\ 0 & 0 & 0 & -1 & -\frac{1}{\tau_f} & \frac{A_b}{\tau_f} & 0 & 0 & 0 & 0 \\ 0 & 0 & -1 & 0 & \frac{B_a}{\tau_f} & -\frac{1}{\tau_f} & 0 & 0 & 0 & 0 \\ 0 & 0 & 0 & 0 & Z_a & Z_b & Z_w & Z_r & 0 & 0 \\ 0 & N_v & N_p & 0 & 0 & 0 & N_w & N_r & 0 & 0 \\ 0 & 0 & 1 & 0 & 0 & 0 & 0 & 0 & 0 & 0 \\ 0 & 0 & 0 & 1 & 0 & 0 & 0 & 0 & 0 & 0 \end{bmatrix} \begin{bmatrix} u \\ v \\ p \\ q \\ a \\ b \\ w \\ r \\ \phi \\ 0 \end{bmatrix} + \begin{bmatrix} 0 & 0 & 0 & 0 \\ 0 & 0 & Y_{ped} & 0 \\ 0 & 0 & 0 & 0 \\ 0 & 0 & 0 & M_{col} \\ \frac{A_{lat}}{\tau_f} & \frac{A_{lon}}{\tau_f} & 0 & 0 \\ \frac{B_{lat}}{\tau_f} & \frac{B_{lon}}{\tau_f} & 0 & 0 \\ 0 & 0 & 0 & Z_{col} \\ 0 & 0 & N_{ped} & N_{col} \\ 0 & 0 & 0 & 0 \\ 0 & 0 & 0 & 0 \end{bmatrix} \begin{bmatrix} \delta_{lat} \\ \delta_{lon} \\ \delta_{ped} \\ \delta_{col} \end{bmatrix}$$

→ 33 parameters, 14 bias values

Measurement equation:

$$\begin{bmatrix} u \\ v \\ w \\ p \\ q \\ r \\ \phi \\ \theta \end{bmatrix} = \begin{bmatrix} 1 & 0 & 0 & 0 & 0 & 0 & 0 & 0 & 0 & 0 \\ 0 & 1 & 0 & 0 & 0 & 0 & 0 & 0 & 0 & 0 \\ 0 & 0 & 0 & 0 & 0 & 0 & 1 & 0 & 0 & 0 \\ 0 & 0 & 1 & 0 & 0 & 0 & 0 & 0 & 0 & 0 \\ 0 & 0 & 0 & 1 & 0 & 0 & 0 & 0 & 0 & 0 \\ 0 & 0 & 0 & 0 & 0 & 0 & 0 & 1 & 0 & 0 \\ 0 & 0 & 0 & 0 & 0 & 0 & 0 & 0 & 1 & 0 \\ 0 & 0 & 0 & 0 & 0 & 0 & 0 & 0 & 0 & 1 \end{bmatrix} \cdot \begin{bmatrix} u \\ v \\ p \\ q \\ a \\ b \\ w \\ r \\ \phi \\ \theta \end{bmatrix}$$

The unknown parameter vector Θ consists of system parameters β , the measurement biases Δz and the trim estimates formulated as input biases Δu [§].

$$\Theta^T = \{\beta^T; \Delta z^T; \Delta u^T\}. \quad (39)$$

The parameters to be estimated are:

L_b : Effect of lateral rotor flapping angle on the lateral moment.

[§] It may not be possible to estimate all the components of Δz and Δu since they could be linearly dependent or highly correlated⁴.

- M_a : Effect of longitudinal rotor flapping angle on longitudinal moment.
- Z_a : Effect of longitudinal rotor flapping angle on vertical force.
- Z_b : Effect of lateral rotor flapping angle on vertical force.
- N_b : Effect of lateral rotor flapping angle on yawing moment.
- A_{lon} : Effect of longitudinal input on lateral rotor flapping angle.
- B_{lat} : Effect of lateral input on longitudinal rotor flapping angle.

The recorded pilot input for the identification maneuvers performed are shown in Figure 5, the maneuvers consist of variable frequency input sweeps on the lateral cyclic and the longitudinal cyclic inputs and are executed manually through a remote control by a trained pilot. Apart from these 6 parameters, 4 input trims, one on each input and two biases (on phi and theta Euler angles) are also estimated. We pay special attention to the performance of the filter in estimating states, filtering noise, and estimating parameters in order to assess the feasibility of the filter to be used in recursive state and parameter estimation applications¹.

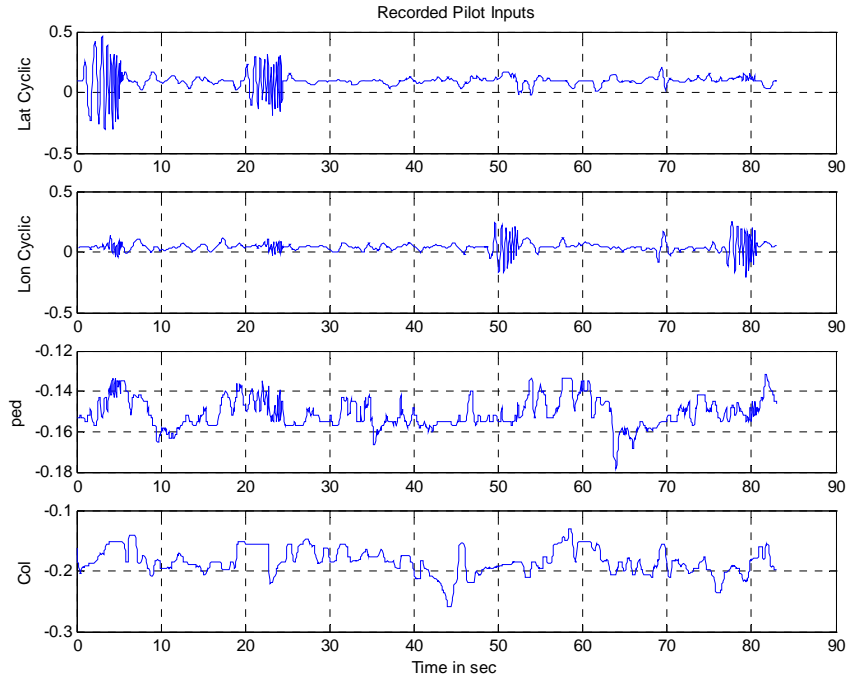


Figure 5 Recorded pilot inputs for ARTIS Sys-ID maneuvers

The EKF state filtering performance is shown in Figure 6, it can be seen that the EKF output matches well with the measured outputs; furthermore the measurement noise is fairly well filtered by the EKF. The S-UKF performs equally well in terms of state filtering, the state filtering performance of S-UKF is seen in Figure 7. The performance of the EKF and the S-UKF is almost identical; this is to be expected since they both assume additive white noise. The augmented UKF, which caters to the case of noise entering nonlinearly in the system, performs marginally better in filtering out the noise in the w (velocity along the body Z axis), the state filtering performance in other channels is almost identical to the other two methods, indicating that additive white noise assumption does not result in great loss of accuracy in the state estimation problem. The state filtering performance of the augmented UKF is shown in Figure 8.

Figure 9: Comparison of recursive parameter estimation algorithms for the ARTIS VTOL UAV, compares the time histories of estimated parameters for the three recursive estimation methods. The parameter estimates from recursive filtering methods do not match well with the offline estimates (estimated using the OEM method and presented in the graph with solid lines), this is mainly accounted to the filtering of process noise in the data by the recursive Kalman filter based methods. The parameter estimates of the EKF and the S-UKF are almost identical

except for the aerodynamic derivative B_{lat} . The same numerical values of Q and R matrices were used for the EKF and the S-UKF case, however different values were required for the augmented UKF case. The augmented UKF was seen to converge the fastest, however it converges to different values than the other two methods. This discrepancy may highlight the effect of nonlinearly entering noise on the performance of recursive parameter estimation algorithms. Table 2 presents the numerical values of the parameters and the percent standard deviation. In all three cases the trim values and the output biases (not shown here) showed rapid convergence to their approximate expected values (approximated from pilot feedback).

The run time of our implementation of the S-UKF algorithm was approximately thrice that of the EKF algorithm, while the run time of the augmented UKF algorithm was approximately six times that of the EKF.

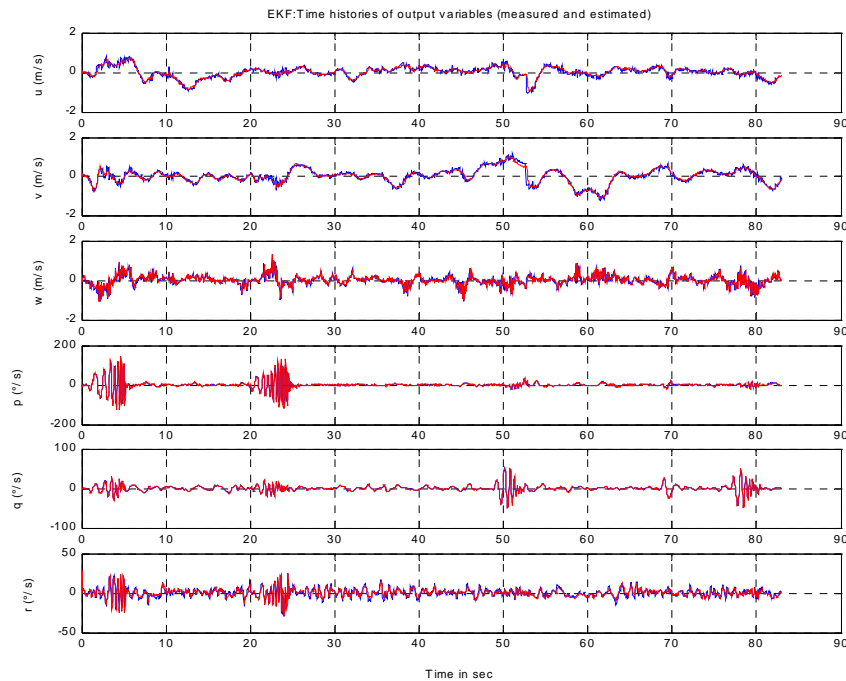


Figure 6: EKF histories of output variables, measured and estimated

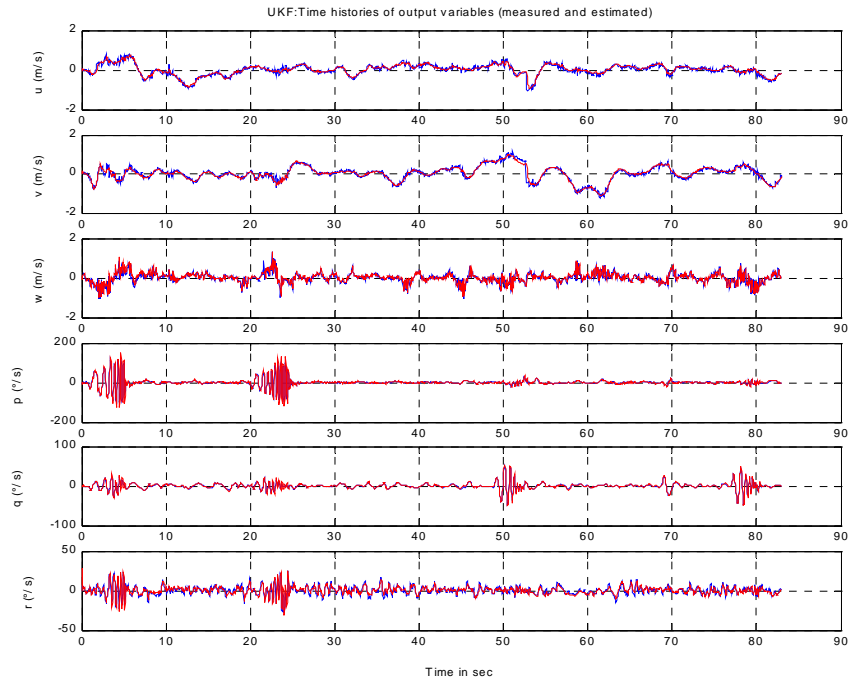


Figure 7: S-UKF time histories of output variables, measured and estimated

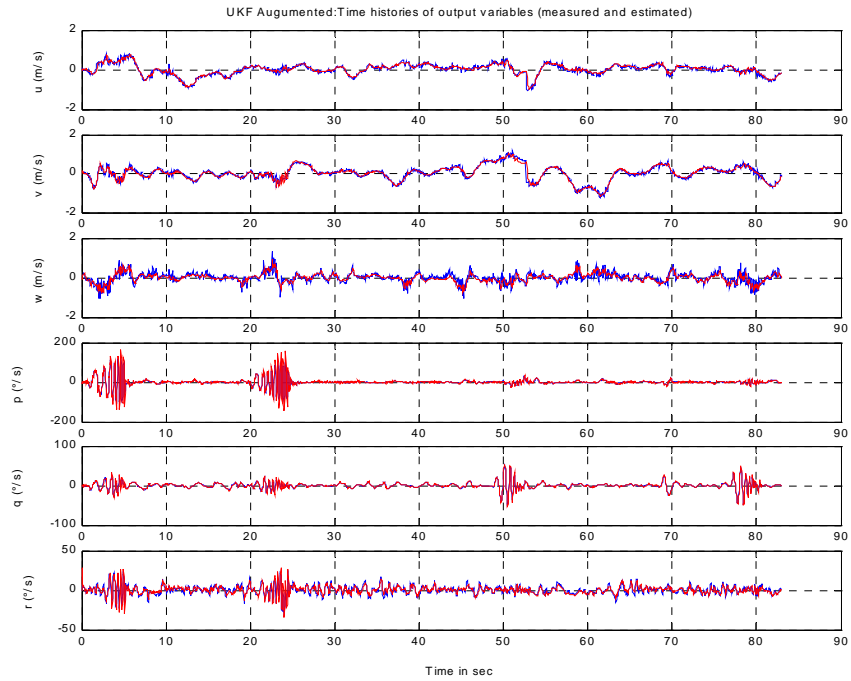


Figure 8: UKF agu: Time histories of output variables, measured and estimated

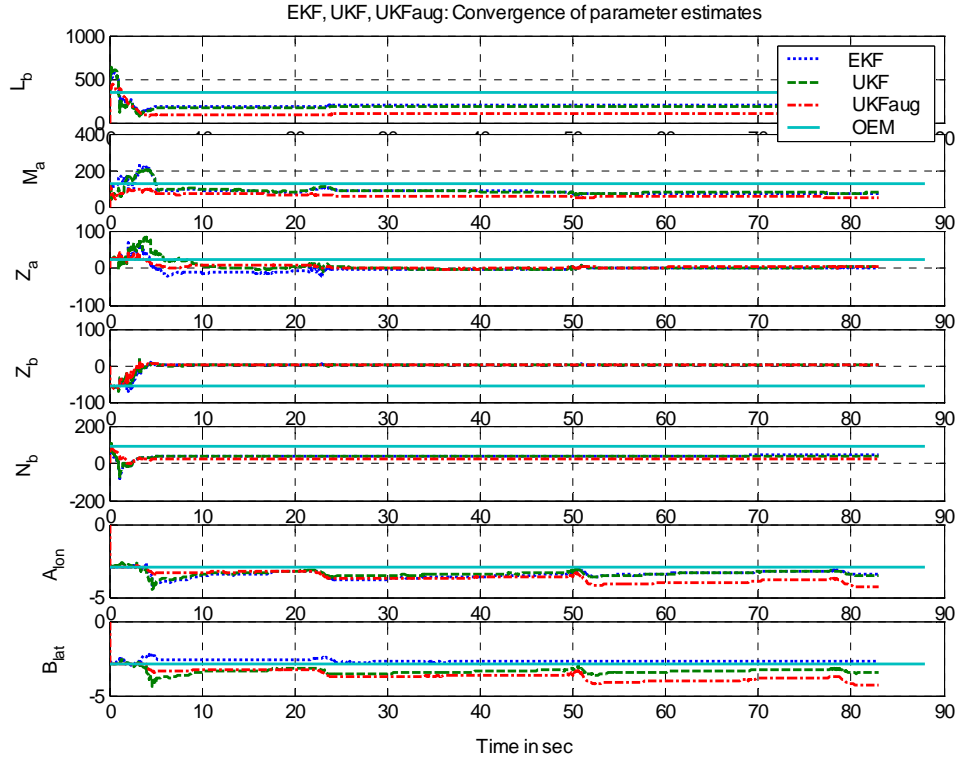


Figure 9: Comparison of recursive parameter estimation algorithms for the ARTIS VTOL UAV

Table 2: Comparison of parameter estimates for the ARTIS VTOL UAV

Parameter	Output error method (FEM)	<i>RPE methods</i>		
		<i>EKF</i>	<i>UKF</i>	<i>UKFaug</i>
L_b	351.294 (0.31)*	205.118 (0.84)	185.691 (0.77)	96.593 (1.41)
M_a	119.2 (0.34)	74.18 (2.20)	77.076 (2.36)	53.35 (5.55)
Z_a	23.284 (8.70)	1.82 (181.17)	5.145 (67.48)	2.955 (48.98)
Z_b	-61.484 (7.66)	3.147 (69.78)	1.160 (184.28)	0.437 (223.16)
N_b	94.049 (1.93)	41.723 (1.05)	41.375 (0.88)	21.122 (2.59)
A_{lon}	-2.626 (0.28)	-3.435 (4.05)	-3.469 (4.01)	-4.27 (11.34)
B_{lat}	-2.357 (0.39)	-2.677 (3.06)	-3.054 (2.70)	-4.101 (7.69)

(*the values in parenthesis denote standard deviation values in percent.)

V. Conclusion

In this paper we compared three recursive parameter identification algorithms for nonlinear filtering of aircraft flight data using three nonlinear recursive parameter estimation algorithms based on Kalman filters:

- 1) The EKF, employing a continuous estimation model with additive noise represented by state vector $x_k^a = [x_k^T \quad \Theta_k^T]^T$; and using a first order approximation for propagation of the covariance matrix,
- 2) General or Augmented case of the UKF employing a continuous estimation model with noise disturbance entering the system nonlinearly, represented by the augmented vector $x_k^a = [x_k^T \quad \Theta_k^T \quad w_k^T \quad v_k^T]^T$, Eqs. (19)-(29), and
- 3) Special or simplified case of the UKF (S-UKF); employing a continuous estimation model with additive noise, represented by state vector $x_k^a = [x_k^T \quad \Theta_k^T]^T$ and to which the simplifications in Eqs. (31) and (32) are used to calculate the covariances.

The results indicate that the UKF augmented recursive parameter estimation method is the fastest in terms of time to convergence. However, it is also the costliest in terms of computational power. The simplified UKF case, which assumes additive uncorrelated noise is equivalent in accuracy and filtering quality with the EKF, and shows little improvement in time to convergence as compared to the EKF. However, even the simplified UKF implementation is computationally more costly than the EKF. The EKF, as expected, maintains excellent filtering quality and decent time to convergence, it is also the computationally least expensive.

For the flight parameter estimation of the HFB-320 research aircraft with a nonlinear estimation model, no great difference between the numerical values of the parameters was seen. This is mainly attributed an accurate estimation model. For the aerodynamic derivative estimation of the ARTIS VTOL UAV; which employs a linear model, considerable discrepancies were seen between the numeric results of the EKF and S-UKF recursive parameter estimation algorithms which assume additive white noise and that of the augmented UKF algorithm which caters to the general case of noise entering nonlinearly. This result highlights the impact of the assumption on how noise enters the system for estimation problems with considerable measurement and process noise coupled with approximate estimation model. Furthermore, the results of the recursive estimation algorithms did not match well with the results of offline output error method results. This discrepancy is mostly attributed to the fact that the OEM method used for offline parameter estimation does not implement filtering of measurement and process noise. It is important to note that the filtering performance of the three algorithms in state estimation was nearly identical.

In conclusion, our results indicate that for flight system parameter identification purposes, the EKF algorithm remains a powerful tool, which consistently returns quality results and is the least costly in terms of computational demand. The UKF algorithm is a theoretically superior alternative to the EKF, however it may not add much to the recursive system identification process if the identification model and the identification data are not appropriate. The UKF is indeed superior in terms of time to convergence, and relative reliability of the estimates, however it is computationally more expensive. Hence, a need is not seen for the replacement of existing EKF based recursive aerodynamic parameter identification algorithms with the UKF. However, it is clear that the UKF is a powerful system identification tool and should be given due attention in the development of future applications involving recursive parameter identification algorithms. Furthermore, the UKF proves itself handy in validating the accuracy of existing EKF based algorithms and improve their performance.

References

- ¹ Chowdhary, G., Lorenz, S., "Control of a VTOL UAV using Online Parameter Identification", AIAA GNC, San Francisco CA, USA 2005
- ² Buckland, J. H., Musgrave, J. L., and Walker, B. K., "On-Line Implementation of nonlinear Parameter Estimation for the Space Shuttle Main Engine", NASA TM-106097, USA 1992.
- ³ Lorenz S., Chowdhary G., "System Identification for a Miniature Rotorcraft, Preliminary Results", AHS 61st forum, Grapevine TX June, 2005
- ⁴ Dittirich J., Bernartz A., Thielecke F. "Intelligent Systems Research using a Small Autonomous Rotorcraft Testbed", 2nd AIAA "Unmanned Unlimited", San Diego CA, September 2003.
- ⁵ Steinber, M. L., "Comparison of Intelligent, Adaptive, and Nonlinear Flight Control Laws", Journal of Guidance, Control and Dynamics, Vol. 24, No. 4, July-August 2001 pp. 693-699.
- ⁶ Song, Y., Campa, G., Napolitano, M., Seanor, B., and Perhinschi, M. G., "On-Line Parameter Estimation Techniques Comparison Within a Fault Tolerant Flight Control System", Journal of Guidance, Control and Dynamics, Vol. 25, No. 3, May-June 200, pp. 528-537.
- ⁷ Gelb A. "Applied Optimal Estimation", MIT press, Massachusetts USA 1974.

- ⁸ Chen, R. T. N., Eulrich, B. J., and Lebacqz, J. V., "Development of Advanced Techniques for the Identification of V/STOL Aircraft Stability and Control Parameters," Cornell Aeronautical Lab., Inc., Report No. BM-2820-F-1, USA 1971
- ⁹ Speyer, J. L., and Crues, E. Z., "On-Line Aircraft State and Stability Derivative Estimation Using the Modified-Gain Extended Kalman Filter," *Journal of Guidance and Control*, Vol. 10, No. 3, 1987, pp. 262-268.
- ¹⁰ Jategaonkar, R., Plaetschke, E., "Estimation of Aircraft Parameters using Filter Error Methods and Extended Kalman Filter", DFVLR FB 88-15, Germany 1988.
- ¹¹ Jategaonkar, R. V., and Plaetschke, E., "Algorithms for Aircraft Parameter Estimation Accounting for Process and Measurement Noise," *Journal of Aircraft*, Vol. 26, No. 4, 1989, pp. 360-372.
- ¹² Garcfa-Velo, J., and Walker, B. K., "Aerodynamic Parameter Estimation for High Performance Aircraft Using Extended Kalman Filtering," *Journal of Guidance, Control, and Dynamics*, Vol. 20, No. 6, 1997, pp. 1257-1259
- ¹³ Julier, S. J., Uhlmann, J. K., and Durrant-Whyte, H. F., "A new Method for the Nonlinear Transformation of Means and Covariances in Filters and Estimators", *IEEE Transactions on Automatic Control*, vol. 45, pp. 477-482, 2000.
- ¹⁴ Julier, S. J., Uhlmann J. K., "Unscented Filtering and Nonlinear Estimation", *Proc. Of the IEEE*, VOL. 92, No. 3, March 2004.
- ¹⁵ Wan, E. A., van der Merwe, R., and Nelson, A. T., "Dual Estimation and the Unscented Transformation", in *Neural Information Processing Systems 12*, 2000, pp. 666-672, MIT Press.
- ¹⁶ Wan, E. A., van der Merwe, R., "The Unscented Kalman Filter for Nonlinear Estimation", Center for Spoken Language and Understanding, OGI school of Science and Engineering, URL: <http://cslu.cse.ogi.edu/nsl/ukf/> [Cited 12th January 2006].
- ¹⁷ Wan, E. A., van der Merwe, R., Julier, S. I., "Sigma-Point Kalman Filters for Nonlinear Estimation and Sensor-Fusion – Applications to Integrated Navigation-", AIAA paper 2004-5120, Aug 2004.
- ¹⁸ Wendel, J., Maier, A., Metzger, J., and Trommer G. F., "Comparision of Extended and Sigma-Point Kalman Filters for Tightly Coupled GPS/INS Integration", AIAA paper 2005-6055, Presented at AIAA GNC, San Francisco CA, USA August 2005.
- ¹⁹ Crassidis, J. L., Markley, F. L., "Unscented Filtering for Spacecraft Attitude Estimation", AIAA Paper 2003-5484, presented at AIAA GNC, Austin TX, USA August 2003
- ²⁰ Brunke, S., Campbell M. E., "Square Root Sigma Point Filtering for Real-Time Nonlinear Estimation", *Journal of Guidance* Vol 27, No. 2, Engineering Notes, pp. 314-317, March 2003
- ²¹ Ljung, L., "Asymptotic Behavior of the Extended Kalman Filter as a Parameter Estimator for Linear Systems", *IEEE Transactions of Automatic Control*, Vol. AC-24, No.1, 1979, pp- 36-50.
- ²² Yuanxin, W., Dewen, H., Meiping, W., Xiaoping, H., "Unscented Kalman Filtering for Additiee Noise Case: Augmented versus Non-augmented", American Control Conference, Portland Oregano, USA 2005.
- ²³ Grewal M., Andrews A., "Kalman Filtering Theory and Practice using MATLAB", Second Edition, John Wiley and Sons, USA 2001
- ²⁴ Bryson, A. E., Ho, Yu-Chi, "Applied Optimal Control: Optimization, Estimation, and Control", Revised Printing, Hemisphere Publishing Corp., USA 1975.
- ²⁵ Gelb, A., "Applied Optimal Estimation", MIT press, Massachusetts USA 1974.
- ²⁶ Mettler, B., "Modeling Identification and Characteristics of Miniature Rotorcrafts", Kluwer Academic Publishers 2003 USA.